Carbohydrate Polymers 149 (2016) 231–241

Contents lists available at ScienceDirect

Carbohydrate Polymers

journal homepage: www.elsevier.com/locate/carbpol

Polysaccharide structures and interactions in a lithium chloride/urea/water solvent

Charles G. Winkworth-Smith*, William MacNaughtan, Tim J. Foster

Division of Food Sciences, School of Biosciences, University of Nottingham, Sutton Bonington Campus, Loughborough LE12 5RD, UK

ARTICLE INFO

Article history:
Received 15 December 2015
Received in revised form 18 April 2016
Accepted 23 April 2016
Available online 11 May 2016

Keywords:
Galactomannan
Konjac glucomannan
Xyloglucan
Cellulose
Lithium chloride
Urea

ABSTRACT

The molten salt hydrate, lithium chloride (LiCl)/urea/water has previously been shown to swell cellulose, but there has so far been no work done to explore its effect on other polysaccharides. In this paper we have investigated the solvent effects of LiCl/urea/water on four natural polysaccharides. Fenugreek gum and xyloglucan, which are both highly branched, were found to increase in viscosity in LiCl/urea/water relative to water, possibly due to the breakage of all intra-molecular associations whereas the viscosity of konjac glucomannan which is predominantly unbranched did not change. Locust bean gum (LBG) had a lower viscosity in LiCl/urea/water compared to water due to the disruption of aggregates. Confocal microscopy showed that fenugreek gum and LBG are able to bind to cellulose in water, however, the conformational change of fenugreek gum in these solvent conditions inhibited it from binding to cellulose in LiCl/urea/water whereas conformational change allowed xyloglucan to bind to cellulose in LiCl/urea/water whilst it was unable to bind in water. Konjac glucomannan did not bind to cellulose in either solvent system. These results provide new insights into the impact of polysaccharide fine structure on conformational change in different solvent environments.

1. Introduction

Hofmeister (1888) was the first to recognise that electrolytes have differing effects on proteins by either increasing their solubility (salting in) or increasing precipitation (salting out). Heydweiller (1910) later discovered that salts dissolved in water increased the surface tension of the solution-air interface where anions were the major influencer. The variation in surface tension followed the Hofmeister series where anions are arranged in order of increasing electrostatic surface potential difference:

$$CO_3^{2-} > SO_4^{2-} > IO_3^- > F^- > BrO_3^- > Cl^- > NO_3^- > Br^- > ClO_3^- > I^- > ClO_4^-$$

The order of some of the cations in the Hofmeister series are:

$$NH_4^+ > K^+ > Na^+ > Li^+ > Mg^{2+} > Ca^{2+}$$

The ions to the left of the series decrease the solubility of nonpoar molecules (salting out) and are referred to as chaotropes as they exhibit weaker interactions with water than water itself and so do not interfere to a great degree with hydrogen bonding whereas the ions with a high charge density, to the right of the series, are refered to as kosmotropes as they exhibit stronger interactions with water molecules than water itself and so are able to break water–water hydrogen bonds.

Kosmotropes are usually small, strongly hydrated ions and are able to structure water, while chaotropes are generally large and poorly hydrated so break the structure of water. A simple method of assessing the nature of an electrolyte is to measure its effect on the viscosity of water. As salt concentrations increase, kosmotropes will increase the viscosity of water whilst chaotropes will decrease it (Wiggins, 2002).

Chloride ions are weakly chaotropic but the behaviour of a halide salt will normally be determined by the stronger metal ion. Therefore, the overall power of a LiCl solution will be kosmotropic. Urea is a chaotrope but acts as a kosmotrope at high concentrations and is able to denature proteins at concentrations of 4–5 M (Russo, 2008). Urea is commonly refered to as a hydrogen bond breaker (Mcgrane, Mainwaring, Cornell, & Rix, 2004). It has been found to increase the intrinsic viscosity of chitosan by breaking intramolecular hydrogen bonds allowing the molecules to exist in a more extended form (Tsaih & Chen, 1997). The concentration of urea required to dis-

* Corresponding author.
E-mail addresses: c.winkworth-smith@nottingham.ac.uk (C.G. Winkworth-Smith), bill.macnaughtan@nottingham.ac.uk (W. MacNaughtan), tim.foster@nottingham.ac.uk (T.J. Foster).

http://dx.doi.org/10.1016/j.carbpol.2016.04.102

rupt the intramolecular hydrogen bonds increased with increasing molecular weight (Chen & Tsaih, 2000).

Urea, as a chaotrope, acts as a co-solvent by promoting a better solvating interaction between the solute and water (Breslow & Guo, 1990). It breaks the structure of water in the bulk and disrupts the hydrophobic parts of non-ionic surfactants (Deguchi & Meguro, 1975). The unfolding process of ribonuclease by urea and LiCl have been compared (Ahmad, 1983). Urea is able to cause complete denaturation where the unfolded molecule acts as a linear random coil whereas the addition of LiCl leads to incomplete unfolding. When low concentrations of LiCl (i.e. below the concentration it is able to denature ribonulcease alone) were added to urea solutions, the salt actually stabilised the protein against urea denaturation (Ahmad, 1984). This may be due to the ability of the carbonyl oxygen of the urea molecules to form strong complexes with the lithium ions.

LiCl/urea/water is a novel molten salt hydrate that has been found to swell cellulose (Tatarova, Manian, Siroka, & Bechtold, 2010) but there has so far been no work done to explore its effect on other natural polysaccharides. Four different polysaccharides, fenugreek gum (FG), locust bean gum (LBG), konjac glucomannan (KGM) and xyloglucan (XG) have been chosen to identify any solvent effects of the LiCl/urea/water solution. The binding of the polysaccharides to cellulose in the different solvent environments has also been investigated.

2. Materials and methods

2.1. Materials

The polysaccharides used were; Konjac glucomannan from the tubers of *Amorphophallus Konjac, K. Koch*: Propol RS (Shimizu Chemical Corporation, Japan), Xyloglucan from tamarind seed (Dainippon Pharmaceutical Company, Japan), Fenugreek Gum Powder T (Air Green Co., Ltd., Japan) and Locust bean gum (Danisco, Norway), all received as kind donations.

The celluloses used were cellulose fibre (Solka 900FCC, International Fibre Corporation, USA) and Avicel MCC type PH-101 Ph Eur (Sigma Aldrich, UK).

LiCl ≥99%, urea, fluorescein isothiocyanate (FTIC) and rhodamine B were purchased from Sigma Aldrich (UK). Dimethyl sulfoxide (99.8%), toluene (99.8%), pyridine (99.5%) were purchased from Acros Organics (UK) and dibutyltin dilaurate (95%) was purchased from Alfa Aesar (UK).

2.2. Sugar analysis

The sugar analysis was carried out by classical methanolysis of polysaccharide followed by trimethylsilyated-derivatization of the released methyl glycosides using the method described by Nagy et al. (2012). Analysis was with Gas Chromatography with a Flame Ionisation Detector (GC-FID).

All samples and standards were dried over phosphorous pentoxide under vacuum. Approximately 5 mg of each sample was weighed out, with the exact weight recorded. Then, to each sample 333 μl of 300 μg/ml sorbitol in anhydrous methanol was added. Following the addition of 666 μl of 3 M methanolic-HCl, the samples were incubated for 5 h at 100 °C. The samples were then dried over a stream of nitrogen and stored in a desiccator under vacuum for 1 h. Subsequently, the samples were mixed with 75 μl pyridine, 75 μl hexamethyldisilazane and 35 μl chlorotrimethylsilane and incubated for 2–3 h and then evaporated to dryness under nitrogen. Finally, 0.6 ml of hexane was added the samples transferred to Eppendorf tubes and centrifuged for 10 min. The clear supernatant was transferred to a GC vial.

GC set-up was as follows; an Agilent HP-1 capillary column (25 m × 0.2 mm × 11 μm) with flame ionisation detection, inlet temperature: 260 °C, FID temp 300 °C, oven gradient 100–150 °C at 10 °C per min – hold 1 min, 150–190 °C at 4 °C per min – hold 5 min, 190–290 °C at 12 °C per min. Helium was used as carrier gas at 0.7 ml/min. Results expressed as grams polysaccharide per 100 g dry weight sample.

2.3. Molecular weight measurement

Molecular weight analysis was carried out with size-exclusion chromatography (SEC)-refractive index detection via the traditional 'peak-position' method, as described by Rieder et al. (2015). Pullulan molar mass standards were used to construct a calibration curve. From this analysis a pullulan relative weight average molar mass was calculated for the entire molar mass distribution.

Approximately 3 mg of each sample was accurately weighed out into 2 ml screw cap microtubes with an O-ring seal, and then wetted with 25 μl 96% v/v ethanol for about 1 h. 2 ml 0.02% sodium azide was added to each tube and the dissolution of the polysaccharide was aided by shaking in a Precellys 24 homogenizer for 3 × 20 s cycles at 5550 rpm. The tubes where then placed in a boiling water bath for 30 min until the polysaccharide had dissolved. Each sample was then filtered through a 0.8 μm syringe filter (Millipore). The HPLC system consisted of two pumps (Dionex P680), a Spectraphysics AS3500 auto injector, a guard-column (Tosoh PWXL), two serially connected columns (Tosoh TSK-gel G6000 PWXL followed by G5000 PWXL, maintained at 40 °C) and a fluorescence detector (Shimadzu RF-10A, Shimadzu, Germany) or a refractive index detector (Shimadzu RID- 6A). The eluent (50 mM Na_2SO_4) was delivered at a flow rate of 0.5 ml/min. Raw data was collected by Chromeleon software v.6.8 (Dionex, USA).

2.4. LiCl/urea/water solution preparation

The swelling solution was prepared with 0.28:0.11:0.61 mol fractions of LiCl, urea and water respectively (Tatarova et al., 2010). The water was added to the dry powders and stirred over heat until the solution turned clear. Any water lost as vapour when solutions were heated was replenished after the solutions were cooled. The final solution had a pH of 6.3.

2.5. Hemicellulose purification and polymer solution preparation

Initially, hemicellulose powders were added to the LiCl/urea/water solution but there was great difficulty in dissolving the hemicelluloses. This may have been due to the small amounts of insoluble impurities present in the samples. The following purification step was then employed:

Hemicellulose stock solutions were prepared by stirring the powders in deionised water and heating to 80 °C for 30 min. The solutions were then left on a roller bed overnight at room temperature. The hemicellulose solutions were then centrifuged at 2000*g* for 40 min at 25 °C. The stock solutions were then diluted to the desired concentration for rheological testing.

Alternatively, the supernatant from the centrifuged polymer stock solutions was freeze dried. The freeze dried material was then dissolved in LiCl/urea/water solution, heated to 80 °C for 30 min and then left on a roller bed overnight at room temperature. The polymer solutions were then diluted to the desired concentration for rheological testing.

2.6. Rapid Visco Analyser (RVA)

Dispersions of cellulose and the polymers in water or LiCl/urea/water were prepared using a Rapid Visco Analyzer (RVA)

(Newport Scientific, Australia) with an initial paddle speed of 200 rpm for 30 s and then at 160 rpm for the remainder of the experiment. The initial temperature was 25 °C which was then increased after 5 min to 90 °C for 10 min (at a heating rate of 6.5 °C min^{-1}) and then cooled back down to 25 °C and held for a further 20 min for a total time of 45 min.

2.7. Rheology

Rheological measurements of the polymer solutions, described in Section 2.5, were carried out using a Bohlin CVO rheometer (Bohlin Instruments Ltd., Cirencester, UK) with cone and plate (4° cone angle/40 mm diameter and 150 μm gap) and double gap (for low viscosity measurements) geometries at 25 °C. Zero shear values were obtained by using the Cross Model within the Bohlin software. Intrinsic viscosities were estimated using the Solomon–Ciuta equation (Solomon & Ciută, 1962):

$$[\eta] = \frac{1}{c}\sqrt{2\left(\eta_{sp} - \ln\eta_{rel}\right)}$$

2.8. Dialysis

Polysaccharide solutions were dialysed after treatment to remove the salts using BioDesignDialysis Tubing (D106) 8000 MWCO (BioDesign Inc., New York, USA). The dialysed samples were then freeze dried to remove water.

2.9. ^{13}C cross polarization magic angle spinning nuclear magnetic resonance (CPMAS NMR)

^{13}C CPMAS NMR spectra were recorded on a Bruker (Karlsruhe Germany) AVANCE 600 NMR Spectrometer with narrow bore magnet and 4 mm triple resonance probe. The parameters used in CPMAS experiments were as follows. The Proton 90° pulse length was 3 μs. Field strength of the proton and spin locking fields during the contact period was 83 kHz. Samples were packed into 4 mm rotors and spun at 10 kHz ppm scales were referenced to the high field peak of adamantane (29.5 ppm) run as an external standard under identical conditions to the samples.

Proton decoupling was provided by a Spinal64 sequence and the proton power levels during the contact time and decoupling stage could be varied independently to provide optimum signal to noise levels. The highest intensity signal for all types of bonded carbons in these carbohydrate materials lay between a contact time of 1 and 2 ms hence for all CPMAS experiments a value of 2 ms was used.

2.10. Fluorescent tagging

LBG and FG were labelled with Rhodamine B, and KGM and XG were labelled with fluorescein isothiocyanate (FTIC). To a two-necked-100 ml-round bottom flask equipped with a magnetic stir bar, the polysaccharide (0.5 g) and fluorescent marker (50 mg) were added. The flask was purged with argon before adding dry dimethylsulfoxide (50 ml) and subsequently attached to the condenser. Pyridine (0.1 ml) and dibutyltin dilaurate (50 mg) were then added to the flask. The reaction was carried out at 95 °C for 24 h. The modified polysaccharide was filtered and washed with ethanol before drying in vacuo.

2.11. Confocal laser scanning microscopy (CLSM)

Polysaccharides were matched to a zero shear specific viscosity of 100 in either water or LiCl/urea/water. 0.01 g of each polysaccharide was replaced with the fluorescently labelled sample. Samples were then run in the RVA. After treatment an aliquot of the sample was deposited onto a glass slide and covered with a cover slip. A Leica TCS SP5 confocal laser scanning microscope (CLSM) was used in single photon mode with an Ar laser with a Leica objective lens (10 × 0.4 IMM/dry/HC PL APO). Different excitation wavelengths were used depending on which florescent sample was used. The excitation wavelengths are 540 nm for rhodamine B and 495 nm for FITC.

Table 1
Sugar analysis with yields described as wt% of dried starting material showing the yields of arabinose (Ara), rhamnose (Rha), fucose (Fuc), xylose (Xyl), glucuronic acid (GlcA), galacturonic acid (GalA), mannose (Man), galactose (Gal) and glucose (Glc).

	Ara	Rha	Fuc	Xyl	GlcA	GalA	Man	Gal	Glc	Sum
LBG	1.8	0.4	0.0	0.9	0.4	1.2	55.1	19.3	1.7	80.8
FG	0.3	0.2	0.0	0.8	0.0	0.6	43.5	39.1	0.4	84.9
KGM	0.0	0.0	0.0	0.4	0.1	0.3	44.1	3.5	26.1	74.5
XG	1.4	0.2	0.0	28.8	0.2	0.6	4.0	14.4	13.2	62.8

2.12. Ball milling

Cellulose fibres were ball milled using a Planetary Mill PULVERISETTE 5 at 200 rpm with 5 min milling followed by a 5 min pause to allow heat to dissipate for a total milling time of 6 h. Each pot (with zirconium balls) was filled with 10 g of cellulose.

3. Results and discussion

3.1. Polysaccharide fine structure and intrinsic viscosity

Sugar analysis gives a clear indication as to the structure of the polysaccharides (Table 1). Galactomannans have a β-1,4-linked mannose backbone with different levels of galactose sidechains. LBG has a mannose to galactose (M:G) ratio of 2.9:1 which is lower than the 4:1 ratio usually found in the literature (Naoi, Hatakeyama, & Hatakeyama, 2002). The M:G ratio of FG is in better agreement with the literature at 1.1:1 (Brummer, Cui, & Wang, 2003; Mathur & Mathur, 2005; Mathur, 2011). Both LBG and FG contain a number of other sugars which may be from a small fraction of other hemicelluloses. The percentage sum of the yield compared to the starting material is in agreement with the amount of insoluble material that is removed during the purification step (≈20 wt%) described in Section 2.

The mannose to glucose ratio of KGM is 1.7:1 which is close to 1.6:1 often described in the literature for the β-(1-4)-linked backbone (Williams et al., 2000). KGM also has a low level of branching (≈8%) at the β-(1-6)-glucosyl units (Nishinari, Takemasa, Zhang, & Takahashi, 2007). There is also small fraction of galactose branching (≈5%) (Buckeridge, Pessoa Dos Santos, & Tiné, 2000).

XG has a cellulosic-like β-1,4-linked glucan backbone highly substituted with α-D-linked xylopyranosyl residues attached at *O*-6 which can be further substituted with other sugar residues. The proportion of glucose from the sugar analysis is much lower than would be expected as it should be at least a little higher than xylose. This is likely to be a result of incomplete acid hydrolysis as the cellulose backbone is much harder to break down than the other sugar side units. This would then explain the low sum value of 62.3% of the dried starting material. This sample of XG has no fucose side units as it is a storage polysaccharide from tamarind seeds rather than from the primary cell wall (Buckeridge, 2010). In aqueous solution this XG will have a flexible random coil configuration (Ren, Picout, Ellis, & Ross-Murphy, 2004).

FG has the highest weight average molecular weight of the polysaccharides used (Table 2) and is larger than LBG although it has a lower intrinsic viscosity in water. These results are in line with some authors such as Brummer et al. (2003) and Wu, Cui, Eskin, and Goff, (2009). Brummer et al. (2003) also found that

Table 2
Molecular weights measured by SEC MALS and intrinsic viscosities measured by rotational rheometry, of each of the polysaccharides. The average of three replicates for each intrinsic viscosity is shown ± the standard deviation.

	Weight average molecular weight (10^6 g/mol)	[η] in Water (dl/g)	[η] in LiCl/urea/water (dl/g)
LBG	2.72	17.5 ± 0.2	10.8 ± 0.1
FG	4.045	15.2 ± 0.1	55.6 ± 2.8
KGM	2.06	15.7 ± 0.4	17.3 ± 0.4
XG	1.48	2.7 ± 0.1	5.1 ± 0.1

LBG had a larger radius of gyration (R_g) than FG. They account for this disparity between molecular weight and intrinsic viscosity by noting previous research which has found that the addition of galactosyl residues on the mannan backbone induces a reduction in chain dimensions (Petkowicz, Reicher, & Mazeau, 1998). Using molecular modelling, Wang and Somasundaran (2007) found that guar gum forms a more compacted helical structure than LBG (which has a stiffer chain) due to the increase in galactose side chains which increases intra-molecular hydrogen bonding. FG is even more highly substituted than guar gum and so is likely to form an even tighter structure.

The intrinsic viscosity of all the polysaccharides is higher in the LiCl/urea/water solvent, except for LBG (Table 2). Goycoolea, Morris, and Gidley (1995) previously found that LBG had an intrinsic viscosity of 12.1 dl/g in 1 M NaCl but this decreased to just 5.2 dl/g in 1 M NaOH. Upon neutralisation the viscosity substantially increased which showed the effects were not wholly due to depolymerisation. They suggested that LBG does not form completely molecular solutions in water but is in fact associated due to the unsubstituted regions of the mannan backbone. These associations or 'hyperentaglements' are broken by alkali resulting in a reduction in viscosity. They showed that guar gum also undergoes a slight decrease in intrinsic viscosity in alkaline conditions from 12.5 to 11.9 dl/g. The decrease is much smaller than for LBG as there are fewer unsubstituted regions on the mannan backbone due to a higher galactose content. Richardson, Willmer, and Foster (1998) found that the addition of sucrose up to a concentration of 10 wt% decreased the intrinsic viscosity of LBG which the authors suggested was due to an decrease in polymer/polymer associations again suggesting that the intrinsic viscosity in water is artificially high due to aggregates. They also found that guar gum was more compact than LBG due to its higher galactose content.

Doyle, Lyons, and Morris (2009), using the same method as Goycoolea et al. (1995) but with FG, found that the addition of 1 M NaOH decreased the intrinsic viscosity from 16.0 to 12.0 dl/g. With increasing NaOH concentration the intrinsic viscosity decreased until levelling off at a concentration of 3 M. This was explained by the alkali causing ionisation of the hydroxyl groups (from —OH to —O^-) which caused electrostatic repulsion and inhibited hyperentanglement. As FG is fully substituted and so does not have any part of the backbone free for mannan–mannan interaction, Doyle et al. (2009) proposed a new theory of hyperentanglement where there are transient associations in the crystallographic *a* plane where galactose side chains lay above or below one another exposing the mannan backbone for weak intermolecular associations as well as the more permanent mannan–mannan associations in the *b* crystallographic plane for less substituted galactomannan.

In this study, the decrease in LBG's intrinsic viscosity is less than might be expected (17.5–10.8 dl/g) when compared to the work of Goycoolea et al. (1995). This might indicate that whilst inter-molecular associations are disrupted there is also a decrease in intra-molecular hydrogen bonding which expands the overall conformation of the individual LBG molecules.

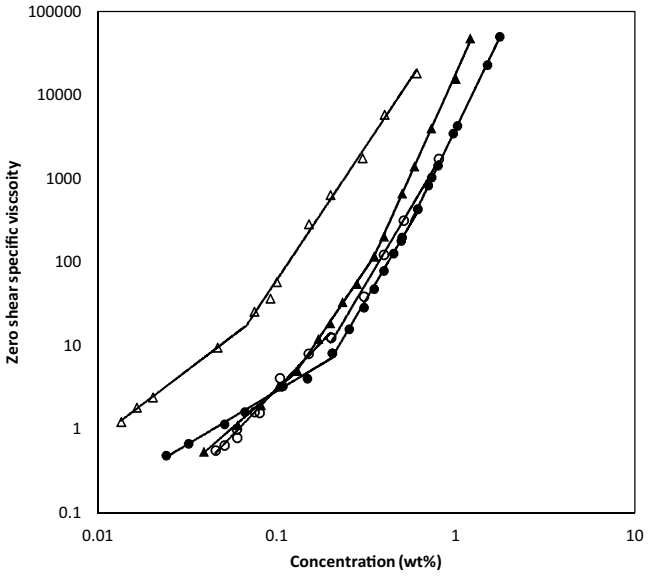

Fig. 1. The zero shear specific viscosity of FG (triangles) and LBG (circles) in water (filled symbols) or the LiCl/urea/water solution (open symbols) at 25 °C.

The work of Doyle et al. (2009) suggests that all the polymers studied in this work may be slightly aggregated in water. However, the increase in intrinsic viscosity of FG, XG and KGM indicates that the conformational change caused by the intramolecular hydrogen bond breaking of LiCl/urea/water creates a larger increase in viscosity than any decrease caused by disaggregation.

KGM has a molecular weight which is in the range that has previously been reported (Dave, Sheth, Mccarthy, Ratto, & Kaplan, 1998; Parry, 2010) (Table 2). KGM is often described as having a semi flexible coil conformation in aqueous solution (Kok, Abdelhameed, Ang, Morris, & Harding, 2009; Li & Xie, 2006) although recent work has suggested that it has an ordered single helix in neutral, dilute solution although at high temperatures (>60 °C), high NaOH (>0.45 M) or high urea (>4.0 M) the order is lost resulting in a random coil conformation (Wang, Zhang, Huang, Chen, & Li, 2011).

Storage xyloglucans are known to have high molecular weights of up to 2×10^6 g/mol (Mishra & Malhotra, 2009). XG decreases in its level of interaction with increased molecular weight (Lima, Loh, & Buckeridge, 2004). Lima et al. (2004) have suggested a mechanism where storage xyloglucans are first synthesised as low molecular weight polymers and then assembled into bigger complexes at the end of polysaccharide deposition.

3.2. Viscosity as a function of concentration

The zero shear specific viscosity of the polysaccharides was compared in pure water and in the LiCl/urea/water solution. Specific viscosity takes into account the differences in the solvent viscosities. By plotting concentration against zero shear specific viscosity on a log–log scale different solution regimes can be differentiated (Mccleary, Clark, Dea, & Rees, 1985). At low concentrations, polymer solutions have no entanglements between molecule chains (Mezger, 2006). At the critical concentration (c^*), there is a pronounced increase in the zero shear specific viscosity, shown by the higher slope, as the polymer chains become entangled.

The viscosity at low concentrations (below 0.1 wt%) of LBG is lower in the LiCl/urea/water solution than in water (Fig. 1) which is in agreement with the decrease in intrinsic viscosity (Table 2). At higher concentrations, LBG's viscosity is similar in both solvents. FG on the other hand has a much higher viscosity in LiCl/urea/water. Similarly XG also has a considerably higher vis-

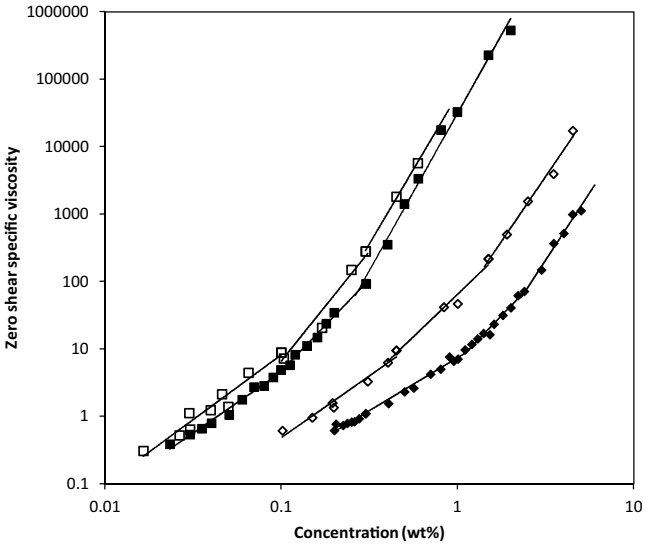

Fig. 2. The zero shear specific viscosity of KGM (squares) and XG (diamonds) in water (filled symbols) or the LiCl/urea/water solution (open symbols) at 25 °C.

cosity in LiCl/urea/water whereas there is only a minimal increase for KGM (Fig. 3 and Table 2).

Aqueous LiCl solutions have previously been found to not affect the intrinsic viscosity of guar gum up to a salt concentration of 4.1 mol/l (Ma & Pawlik, 2007). However, a saturated solution of LiCl increased the intrinsic viscosity of guar gum from 11.7 to 21.7 dl/g. Urea had no effect on the intrinsic viscosity up to a concentration of 1 mol/l but at 4 mol/l concentration the intrinsic viscosity increased to 14.5 dl/g although, interestingly, the intrinsic viscosity decreased slightly for a saturated urea solution. Saturated solutions of cesium chloride (CsCl) decreased guar gum's intrinsic viscosity. Ma and Pawlik (2007) account for these differences by the solvent quality of the different salt solutions. Saturated CsCl (a chaotrope and thus a water-structure breaker) is a better solvent than water so fully solubilises guar gum by dissociating any aggregates between the unsubstituted mannan chains. They suggest that saturated LiCl and NaCl (kosmotropes) solutions actually increase the level of aggregation by the Li^+ and Na^+ binding water molecules into their hydration sheaths leaving little water to hydrate/solubilise the polymer chains thereby making polymer–polymer interactions more favourable than polymer-solvent interactions. This competitive hydration model does not correlate, however, with their results for urea. They suggest that the hydrogen bond breaking properties of urea do not occur at the low concentrations of guar gum they studied. The authors exclude conformation change as a possible cause in altering the intrinsic viscosity due to the non-ionic nature of guar gum and so insist there can be no screening of anionic functional groups.

Recently, researchers have begun to dispute the idea that water structure breaking and making is central to the Hofmeister series (Zhang & Cremer, 2006) and that rather, direct ion-macromolecule interactions are the major driving force. Using femto-second mid-infrared pump-probe spectrocopy, Omta, Kropman, Woutersen, and Bakker (2003) found that the water structure outside the hydration shell of the ion was not influenced by the ion.

A model of hydrogen bond breaking causing conformational change gives a more complete picture of what may be happening in both the present paper and the work of Ma and Pawlik (2007). We believe that the intrinsic viscosity of LBG does decrease in LiCl/urea/water due to the break-up of aggregates but conformational change increases the viscosity of FG and XG. If competition for water was the major factor then KGM should also increase in viscosity to a similar level, but it does not as it does not undergo significant conformational change, which appears to be caused by the excessive sidechain branches of the FG and XG.

β-1,4 glucans, β-mannans and β-xylans cause a much greater reduction in the freedom of movement of water molecules than α-galactans, α-mannans, α-xylans and α-glucans, which results in their surface minimisation and concomitant reduction in water solubility (Chaplin, 2003). Hydrophobic molecules prefer a less dense aqueous environment than hydrophilic molecules. The low density of water is therefore a good solvent for hydrophobic molecules as they need to order the water around them which tends to happen at low temperatures (Chaplin, 2000, 2001). Xylose units are more hydrophobic than galactose or glucose as they have one less OH group (Picout, Ross-Murphy, Errington, & Harding, 2003). With the removal of some galactose side chains (>35%) using fungal β-galactosidase, concentrated XG solutions are able to gel at high temperature due to the aggregation of hydrophobic domains to minimise the hydrophobic surface area in contact with the bulk water (Brun-Graeppi et al., 2010). The mannan backbone of FG is sheilded by the galactose side chains resulting in the backbone being hydrophobic (Dionísio & Grenha, 2012; Mathur, 2011).

Urea is able to disrupt hydrophobic interactions by disordering water structure (de Xammar Oro, 2001) although the influence of urea on hydrophobic interactions is controversial (Cho, Heuzey, Bégin, & Carreau, 2006). Urea at a concentration of 7 M was able to disrupt the hydrophobic domains of chitosan (Philippova et al., 2001). Urea may therefore be causing conformational change by both breaking hydrogen bonds and disrupting the hydrophobic domains of both FG and XG which leads to the large increase in viscosity.

3.3. Solid state NMR analysis

Ivory nut mannan is an example of nearly pure mannan (Putaux, 2005). It is insoluble in water which is usually attributed to the strong mannan–mannan intermolecular associations. With increasing galactose content these interactions are weakened by the steric hindrance of the side units which increases aqueous solubility. LBG is able to form gels following a freeze-thaw treatment whereas the more highly substituted guar is not. Similarly to cellulose, mannan I is the native crystalline state which can be converted to mannan II after alkali treatment (Chanzy, Dube, Marchessault, & Revol, 1979) although mannan II is also found in nature (*Codium fragile*) (Marchessault, Taylor, & Winter, 1990). In contrast with cellulose, native crystal forms of mannan have an anti-parallel chain packing of two-fold helices (Chanzy, Perez, Miller, Paradossi, & Winter, 1987). All galactomannans, regardless of their level of substitution have a broadly similar three-dimensional crystal structure with an anti-parallel sheet stabilised by mannan–mannan hydrogen bonding (Song, Winter, & Taravel, 1989). Any spaces where a galactose molecule would otherwise be will be filled by a water molecule and thus a loss in crystallinity upon drying is found due to a collapse in the structure. Due to fenugreek's higher galactose substitution it shows markedly less loss of crystallinity upon drying than LBG, tara or guar (Song et al., 1989).

^{13}C CPMAS NMR is primarily used to identify order at the molecular level rather than crystalline structure (Gidley, Mcarthur, & Underwood, 1991). Gidley et al. (1991) compared guar gum, LBG and KGM using ^{13}C CPMAS NMR. They found that all the dry samples (8–10 wt% H_2O) had broad spectral features with only limited resolution of signals (i.e. amorphous) and that hydration (30 wt%) led to narrower resonances and increased resolution. This hydration-induced conformational adjustment has also been seen for other polysaccharides such as agarose and kappa- and iota-carrageenan (Saitô, Yokoi, & Yamada, 1990). Ivory nut mannan, however, does have sharp resonances for the dry powder. These sharp signals are

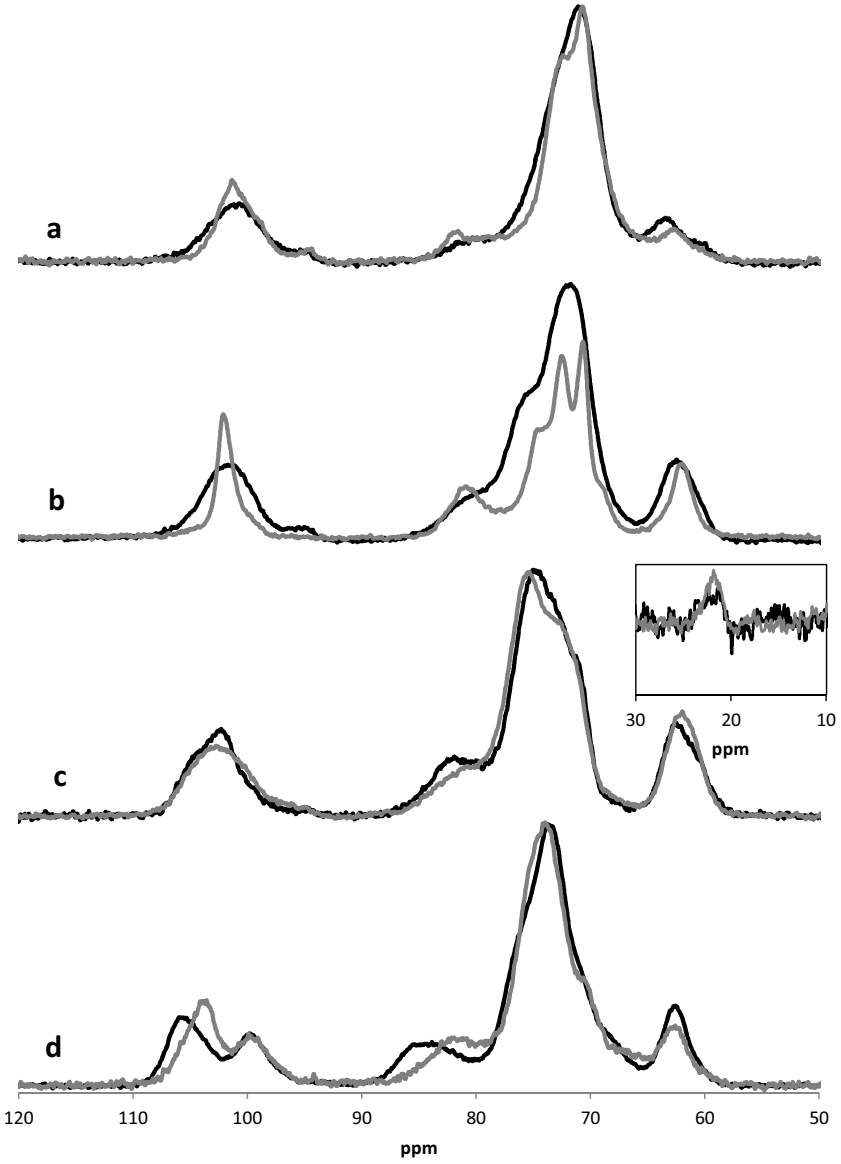

Fig. 3. ^{13}C CPMAS NMR spectra of polysaccharide samples that were either treated in LiCl/urea/water and dried (grey) or untreated (black), for (a) FG (b) LBG (c) KGM and (d) XG. Insert graph shows the acetyl methyl region for LiCl/urea/water treated (grey) and untreated (black) KGM.

consistent with the crystalline nature of the mannan which has also been found with X-ray diffraction (XRD) (Atkins, Farnell, Burden, Mackie, & Sheldrick, 1988). Hydration broadened these features in CPMAS NMR and XRD which indicated a decrease in both crystalline and molecular order (Gidley et al., 1991).

Samples of the treated and untreated polysaccharides were dialysed to remove the solvent and freeze dried. The ^{13}C CPMAS NMR spectrum of the treated FG sample has slightly more resolved peaks than those of the untreated sample (Fig. 3a) which indicates there was a small increase in molecular order. Whilst FG generally has a M:G ratio of 1:1 (Mathur & Mathur, 2005), in this study it was found to be slightly higher at 1.11:1 (Table 6.2), which suggests 48% galactose substitution. Consequently, there may be enough free mannose to allow slight hydrophobic ordering as the FG contracts upon solvent removal which may cause minor aggregation.

The NMR spectra show a large difference between the treated and untreated LBG samples (Fig. 3b). Although both samples were in pure aqueous solution before drying, as all the salts should have been removed by dialysis, the treated LBG sample appears to have much greater molecular order than the untreated sample as shown by the sharper peaks. The spectrum seen in Fig. 3b for the treated LBG is very similar to that of mannan II from *Codium fragile* (Marchessault et al., 1990). This could be interpreted as the galactose residues being removed during treatment leaving behind almost pure mannan chains that are able to crystallise but this is not born out from the FTIR spectra (results not shown) where there is almost no change, implying that there has been very little, if any, chemical modification. As seen by the decrease in intrinsic viscosity the LBG aggregates are broken by the LiCl/urea/water solvent. When the solvent is replaced by water these smaller LBG units will once again aggregate due to the unsubstituted regions on the LBG mannan backbone which are hydrophobic (Picout et al., 2003). A process similar to crystallisation can be envisaged whereby, due to the smaller starting size, the LBG units can fit together more efficiently to produce aggregates with greater molecular order. By a possible analogous mechanism, β-glucans have been found to gel faster and produce gels with greater G′ values as the molecular weight decreases (Brummer et al., 2014).

During dialysis with deionised water of the treated KGM, the sample underwent gelation. Gelation of KGM can be achieved by

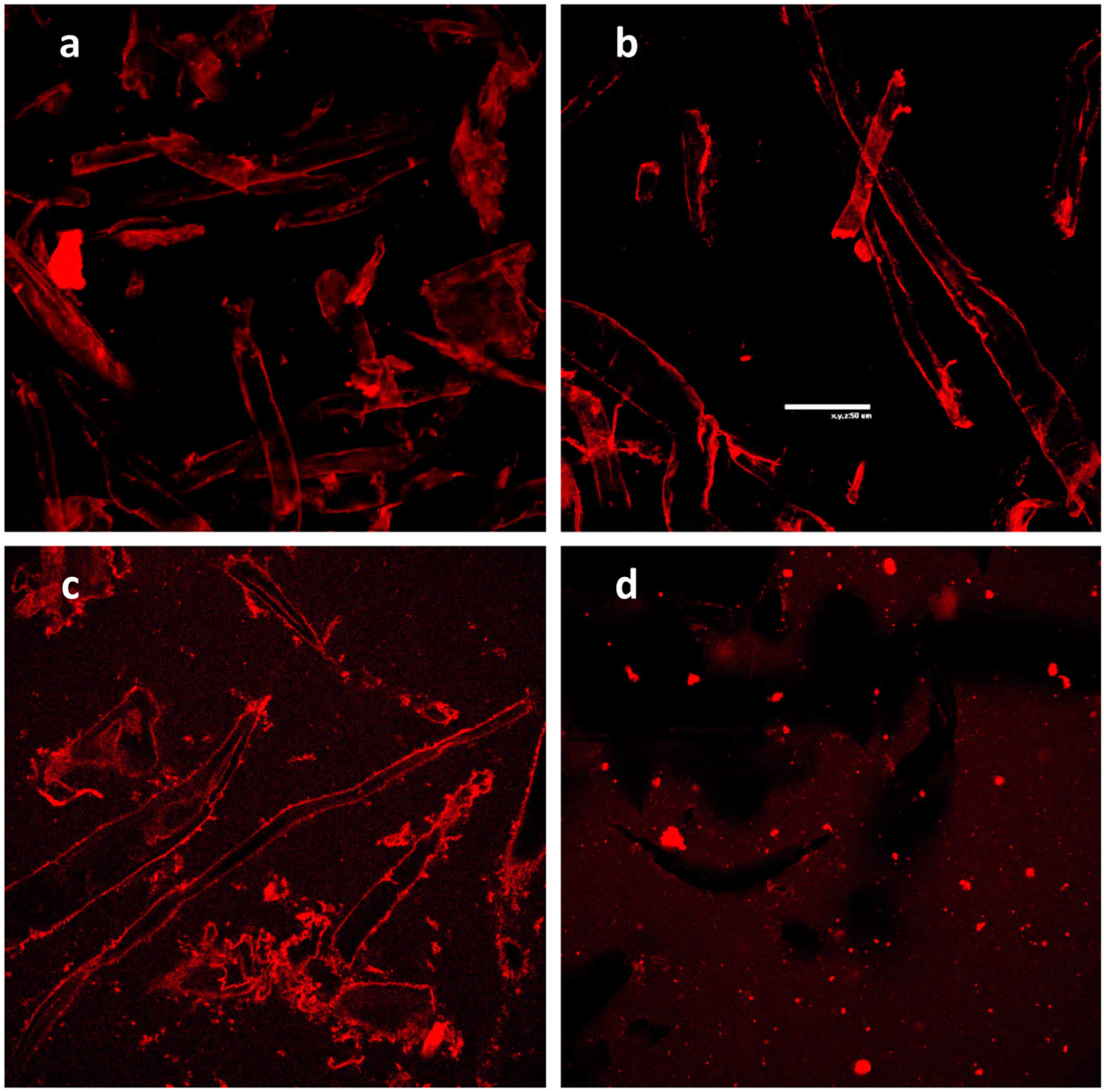

Fig. 4. Confocal micrographs showing galactomannans and cellulose fibres in different solvents (a) LBG in water (b) FG in water (c) LBG in LiCl/urea/water solution and (d) FG in LiCl/urea/water solution. Scale bar is 50 μm.

alkali treatment, causing deacetylation (Penroj, Mitchell, Hill, & Ganjanagunchorn, 2005). This does not appear to be the cause of gelation for this system as the pH of the LiCl/urea/water solution was 6.3 and gelation occurred during the removal of the salts. The insert graph in Fig. 3 shows acetyl carbon peaks for both the untreated and treated KGM samples at 22 ppm (Bootten, Harris, Melton, & Newman, 2004). While the spectra are noisy the peaks appear to be the same size for both samples which indicates that the acetyl groups have not been removed during treatment. Yin, Zhang, Huang, and Nishinari (2008) found that the addition of a salting in salt suppressed KGM gelation but lower salt concentrations assisted gelation. As the LiCl and urea concentrations decreased during dialysis, the salting in power of LiCl was likely overpowered by the salting out effect of urea at low concentrations which promoted gelation. Although KGM did produce order (gel) during dialysis the order was lost upon drying as there is little difference in the NMR spectra of the treated and untreated samples (Fig. 3c).

For XG the peak at 99–100 ppm can be assigned to the xylose C1 (Bootten, Harris, Melton, & Newman, 2008; Whitney, Brigham, Darke, Reid, & Gidley, 1995) and does not shift for the treated samples (Fig. 3d). The chemical shift at 82.5 ppm is assigned to the C4 glucan chain (Ha, Apperley, & Jarvis, 1997). The peak at 105.8 ppm for the untreated XG, which corresponds to the C1 (1,4-Glc) region of the glucose backbone (Dick-Pérez et al., 2011), shifts to 103.8 ppm after treatment. A parallel can be drawn from starch as the major peak in the C1 region of starch is known to shift from about 102 ppm to 105 ppm as it becomes more amorphous (Gidley & Bociek, 1988; Gidley, 1992). The addition of the LiCl/urea/water will break the intra-molecular hydrogen bonding which will allow the cellulosic backbone to have a flatter, more extended conformation. As the salt is removed by dialysis the XG chains may aggregate in a more uniform way due to the extended conformation, which is shown by the increase in molecular order from the NMR results.

A crucial aspect of the interpretation of data of this type is whether the solutions formed on dissolution are truly molecular or are still in the form of aggregates. This is a difficult point to definitively answer and from the available evidence general indications only can be given. One argument for the formation of solutions at the molecular level, at least in the case of the LiCl/urea/water system lies in the interpretation of these high resolution solid state measurements (Fig. 3). They are sensitive to order at a local level. The samples have been “dissolved” in both solvents, namely

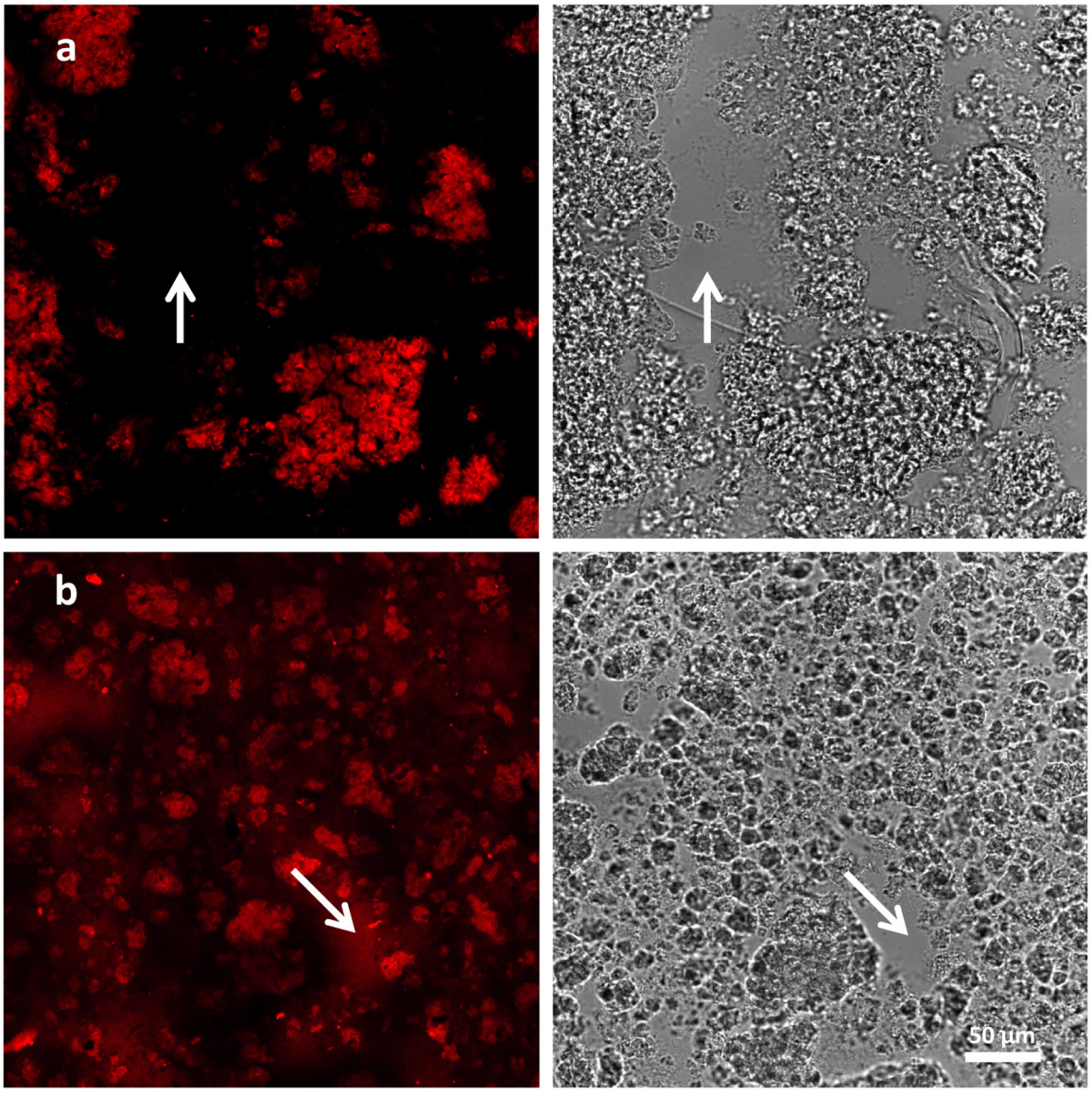

Fig. 5. Confocal micrographs of ball milled MCC in LiCl/urea/water with (a) LBG and (b) FG. The light micrographs of the same image are shown on the right. The arrows point to a part of each image where there is no cellulose.

LiCl/urea/water and water alone and then dialysed and freeze dried. The fact that the LiCl/urea/water samples invariably show higher local order (higher resolution spectra) implies that these samples have reassembled from a more primitive form which we propose is most likely to be a molecular or close to molecular solution. The samples dissolved in water could have behaved similar to this proposal or have been aggregates and remained so during the process. This is not unequivocal as reassembly could have occurred during the drying process in the case of the LiCl/urea/water by molecular rearrangements, however it is more suggestive of a system which has gone to the molecular level at least for the samples in the LiCl/urea/water system but not necessarily for the samples dissolved in water. It is partly for this reason that the solid state results are important to this work.

FTIR (results not shown) measurements suggest that none of the polysaccharides undergo any chemical modification during treatment indicating that the differences seen between the solvents are as a result of conformational changes. FG has the largest molecular weight of the polysaccharides tested yet has a comparatively low viscosity in water; due to its high level of galactose substitution it has a very compacted structure as the galactose side chains form intramolecular hydrogen bonds (Petkowicz et al., 1998; Wang & Somasundaran, 2007). When dissolved in the LiCl/urea/solvent these intra-molecular hydrogen bonds are broken which allows the molecular conformation to expand leading to a large increase in intrinsic viscosity. The inter-molecular associations between LBG molecules are broken, resulting in a decrease in intrinsic viscosity. Whilst the number of intra-molecular hydrogen bonds is less for LBG due to the low number of galactose side chains, their breakage results in a slight expansion which explains why there is no overall decrease in viscosity at semi-dilute and concentrated solution regimes. KGM is a linear molecule with only a very low level of branching which may explain why there is only a slight increase in the viscosity in LiCl/urea/water. XG is highly branched and thus has a compacted conformation. It behaves in a similar way to FG in the LiCl/urea/water solvent where intra-molecular hydrogen bonds are broken and hydrophobic regions are disrupted resulting in a large increase in viscosity.

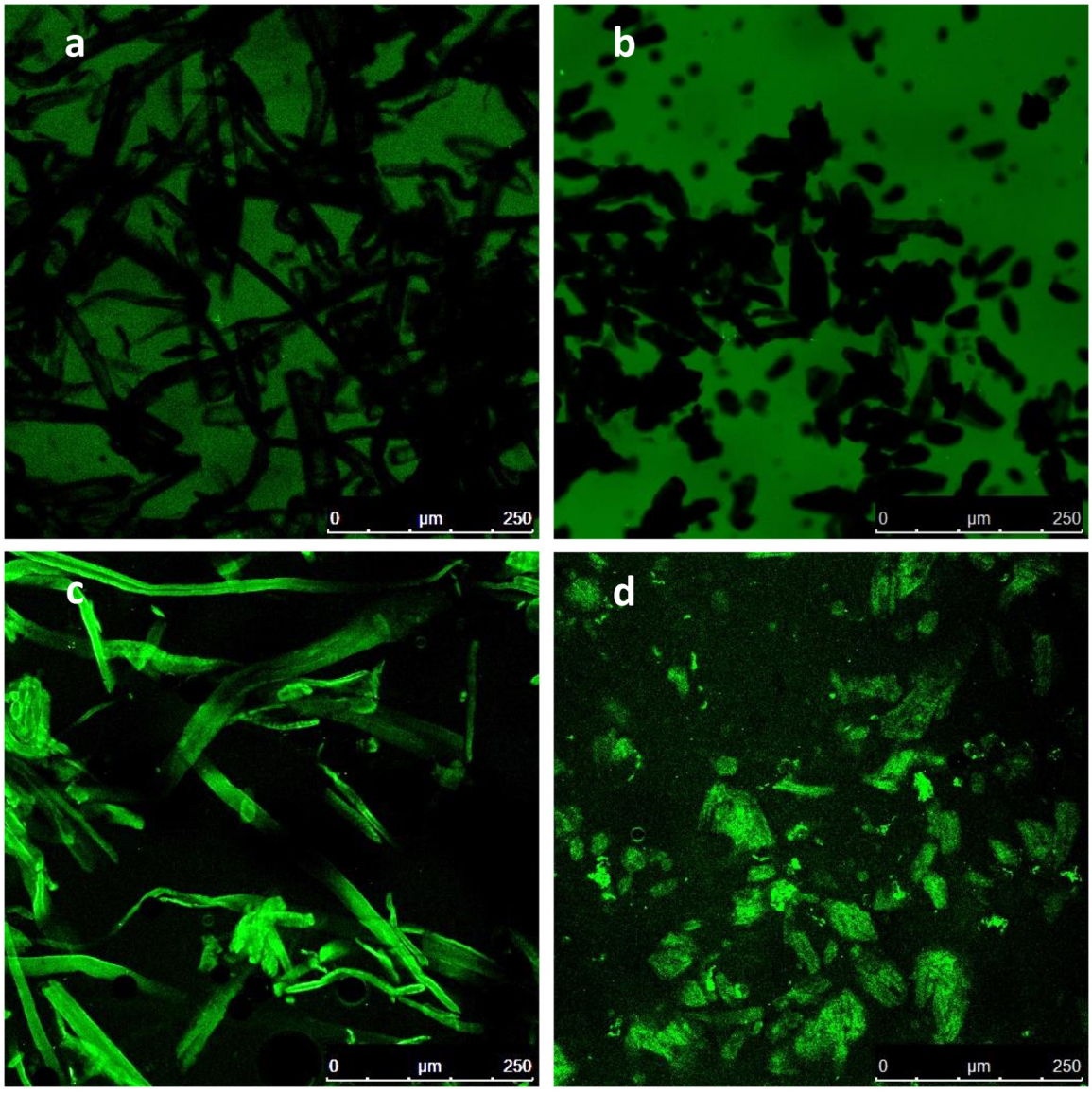

Fig. 6. Confocal micrographs showing XG with (a) cellulose fibres and (b) MCC in water and XG with (c) cellulose fibres and (d) MCC in LiCl/urea/water.

3.4. Cellulose and polysaccharide interactions

Figs. 4–6 show confocal micrographs of fluorescently labelled polysaccharides with cellulose in either water or LiCl/urea/water. There will be a proportion of the polysaccharides in solution that are not bound to the cellulose; however, when polysaccharides are bound to the surface of the cellulose, they are far more concentrated and reveal the outline of the cellulose. When unbound, the surrounding solution appears brighter on the micrographs.

Fig. 4 shows confocal micrographs of cellulose fibre and LBG or FG. In water both LBG and FG (Fig. 4a and b) appear to bind to the surface of the cellulose fibres. With no quantitative values it is not possible to state if there is any difference between the two galactomannans. Whitney, Brigham, Darke, Reid, and Gidley, (1998) used bacterial cellulose to investigate interactions between cellulose and mannans. They found that galactomannan interaction followed the order of galactose substitution, so that LBG with the lowest substitution had greater interaction than the fully substituted FG indicating that the galactosyl substitution was a significant barrier to association with cellulose fibrils. The unsubstituted mannan backbone was able to adopt the extended cellulose conformation so LBG was also able to form cross-links between the cellulose fibrils.

From the work of Whitney et al. (1998) it would be expected that FG would bind to a much lesser degree than LBG but visually there appears to be little difference between the galactomannans. In the LiCl/urea/water solution LBG is still bound to the cellulose (Fig. 4c) whereas there seems to be no interaction between the FG and cellulose (Fig. 4d). It should be noted, however, that the fluorescently labelled FG was far less soluble in LiCl/urea/water which can be seen by the bright specs.

Now investigating the interaction between LBG and FG with physically processed ball milled microcrystalline cellulose (MCC), LBG and FG both appear to bind in LiCl/urea/water (Fig. 5). The arrows point to a part of each image where there is no cellulose. For the LBG sample this area is dark as the majority of the LBG has bound to the cellulose whereas in the FG sample there is still a significant amount of polymer that is not bound.

In this study, in water, XG does not bind to either cellulose fibres (Fig. 6a) or MCC (Fig. 6b). This is likely due to the absence of fucose side chains (Table 1) which have been shown to aid interaction due to the flatter conformation on the main chain (Hayashi, Ogawa, &

Mitsuishi, 1994; Levy, York, Stuikeprill, Meyer, & Staehelin, 1991). XG has a tightly bound conformation in water but in LiCl/urea/water the side chains unfold as intramolecular hydrogen bonds are broken. This exposes the glucose backbone and enables the XG to bind to cellulose (Fig. 6c and d). de Lima and Buckeridge (2001) found there was a slightly higher interaction between cellulose and XG at a pH of 6.0 (between the range of pH 2–8) whilst temperature had no effect between the range of 5–60 °C. The pH of the LiCl/urea/water solvent is 6.3 so the change in pH may also increase the level of binding of XG but this is unlikely to be the sole reason, as the increase found by de Lima and Buckeridge (2001) was small.

Due to problems drying the fluorescently labelled KGM there was a large amount that remained undissolved. It is therefore difficult to be completely confident with the images. However, the confocal micrographs that were taken (please see supplementary material) appear to suggest that KGM does not bind to cellulose in either water of LiCl/urea/water. As there are minimal solvent effects for KGM (Fig. 2), it might be expected that it would behave in a similar manner in both solvents.

These results suggest that changes in polysaccharide structure influenced by solvent type affects their interaction with cellulose. The confocal micrographs only provide a qualitative understanding of the polymer-cellulose binding so it would be useful to quantify this in future work. This could be achieved using the method of Mishima, Hisamatsu, York, Teranishi, and Yamada (1998) where they packed columns with cellulose and solutions of each polysaccharide were then applied to the column and the amount of carbohydrate eluted was measured calorimetrically.

4. Conclusion

LiCl/urea/water appears to be able to break both intra- and intermolecular hydrogen bonds and disrupts hydrophobic domains. This may result in the conformational change from tightly bound and compact in water to a more extended conformation in LiCl/urea/water for FG and XG, which are both highly branched. LBG aggregates are also broken lowering its intrinsic viscosity. However, at high concentrations the expansion of the smaller molecules results in no overall change in viscosity. KGM, which is only minimally branched, does not undergo any significant conformational change from water to LiCl/urea/water.

Both the fluorescently labelled LBG and FG bind to cellulose in water. The conformational change of FG in LiCl/urea/water seems to inhibit binding to cellulose whereas XG does bind to cellulose in LiCl/urea/water but does not in water. These results therefore indicate that the binding to cellulose is not described by simple molecular models, and may vary as a function of polymer, which will be a result of both polymer conformation and also fine structure and side chain distributions and lengths. The results of KGM binding are inconclusive but suggest that it does not bind to cellulose in either water or LiCl/urea/water. It is, however, unclear as to what effect the fluorescent labelling may have on the properties of these polysaccharides so further work needs to be done using alternative fluorescent markers to confirm the results. The solvent induced conformational change described in this work may provide new routes to structure formation with cellulose.

LiCl/urea/water is a useful solvent for hemicelluloses as it disrupts many of the intra-molecular associations. Branched polysaccharides therefore may have a larger hydrodynamic volume resulting in a higher viscosity when compared to water whilst disaggregation will result in a reduction in viscosity.

Acknowledgements

This research was financially supported by the Engineering and Physical Sciences Research Council (EPSRC) and Unilever. Fluorescent tagging was kindly carried out by Latifah Jasmini (Chemical Engineering, University of Nottingham). Sugar analysis and molecular weight measurements were kindly performed by Nofima (Norway).

Appendix A. Supplementary data

Supplementary data associated with this article can be found, in the online version, at http://dx.doi.org/10.1016/j.carbpol.2016.04.102.

References

Ahmad, F. (1983). Free energy changes in ribonuclease A denaturation. Effect of urea, guanidine hydrochloride, and lithium salts. *Journal of Biological Chemistry*, *258*, 3–11146.

Ahmad, F. (1984). Free energy changes in denaturation of ribonuclease A by mixed denaturants. Effects of combinations of guanidine hydrochloride and one of the denaturants lithium bromide, lithium chloride, and sodium bromide. *Journal of Biological Chemistry*, *259*, 4183–4186.

Atkins, E., Farnell, S., Burden, C., Mackie, W., & Sheldrick, B. (1988). Crystalline structure and packing of mannan I. *Biopolymers*, *27*, 1097–1105.

Bootten, T. J., Harris, P. J., Melton, L. D., & Newman, R. H. (2004). Solid-state ^{13}C NMR spectroscopy shows that the xyloglucans in the primary cell walls of mung bean (*Vigna radiata* L.) occur in different domains: a new model for xyloglucan–cellulose interactions in the cell wall. *Journal of Experimental Botany*, *55*, 571–583.

Bootten, T. J., Harris, P. J., Melton, L. D., & Newman, R. H. (2008). WAXS and ^{13}C NMR study of Gluconoacetobacter xylinus cellulose in composites with tamarind xyloglucan. *Carbohydrate Research*, *343*, 221–229.

Breslow, R., & Guo, T. (1990). Surface tension measurements show that chaotropic salting-in denaturants are not just water-structure breakers. *Proceedings of the National Academy of Sciences of the United States of America*, *87*, 167–169.

Brummer, Y., Cui, W., & Wang, Q. (2003). Extraction: purification and physicochemical characterization of fenugreek gum. *Food Hydrocolloids*, *17*, 229–236.

Brummer, Y., Defelice, C., Wu, Y., Kwong, M., Wood, P. J., & Tosh, S. M. (2014). Textural and rheological properties of oat beta-glucan gels with varying molecular weight composition. *Journal of Agricultural and Food Chemistry*, *62*, 3160–3167.

Brun-Graeppi, A. K., Richard, C., Bessodes, M., Scherman, D., Narita, T., Ducouret, G., et al. (2010). Study on the sol–gel transition of xyloglucan hydrogels. *Carbohydrate Polymers*, *80*, 555–562.

Buckeridge, M. S., Pessoa Dos Santos, H., & Tiné, M. A. S. (2000). Mobilisation of storage cell wall polysaccharides in seeds. *Plant Physiology and Biochemistry*, *38*, 141–156.

Buckeridge, M. S. (2010). Seed cell wall storage polysaccharides: models to understand cell wall biosynthesis and degradation. *Plant Physiology*, *154*, 1017–1023.

Chanzy, H., Dube, M., Marchessault, R., & Revol, J. (1979). Single crystals and oriented crystallization of ivory nut mannan. *Biopolymers*, *18*, 887–898.

Chanzy, H., Perez, S., Miller, D. P., Paradossi, G., & Winter, W. T. (1987). An electron diffraction study of the mannan I crystal and molecular structure. *Macromolecules*, *20*, 2407–2413.

Chaplin, M. (2000). A proposal for the structuring of water. *Biophysical Chemistry*, *83*, 211–221.

Chaplin, M. F. (2001). Water: its importance to life. *Biochemistry and Molecular Biology Education*, *29*, 54–59.

Chaplin, M. F. (2003). Fibre and water binding. *Proceedings of the Nutrition Society*, *62*, 223–227.

Chen, R. H., & Tsaih, M. L. (2000). Urea-induced conformational changes of chitosan molecules and the shift of break point of Mark–Houwink equation by increasing urea concentration. *Journal of Applied Polymer Science*, *75*, 452–457.

Cho, J., Heuzey, M.-C., Bégin, A., & Carreau, P. J. (2006). Effect of urea on solution behavior and heat-induced gelationof chitosan-β-glycerophosphate. *Carbohydrate Polymers*, *63*, 507–518.

Dave, V., Sheth, M., Mccarthy, S. P., Ratto, J. A., & Kaplan, D. L. (1998). Liquid crystalline: rheological and thermal properties of konjac glucomannan. *Polymer*, *39*, 1139–1148.

Deguchi, K., & Meguro, K. (1975). The effects of inorganic salts and urea on the micellar structure of nonionic surfactant. *Journal of Colloid and Interface Science*, *50*, 223–227.

Dick-Pérez, M., Zhang, Y., Hayes, J., Salazar, A., Zabotina, O. A., & Hong, M. (2011). Structure and interactions of plant cell-wall polysaccharides by two-and three-dimensional magic-angle-spinning solid-state NMR. *Biochemistry*, *50*, 989–1000.

Dionísio, M., & Grenha, A. (2012). Locust bean gum: exploring its potential for biopharmaceutical applications. *Journal of Pharmacy & Bioallied Sciences*, *4*, 175.

Doyle, J. P., Lyons, G., & Morris, E. R. (2009). New proposals on hyperentanglement of galactomannans: solution viscosity of fenugreek gum under neutral and alkaline conditions. *Food Hydrocolloids*, *23*, 1501–1510.

de Xammar Oro, J. R. (2001). Role of co-solute in biomolecular stability: glucose, urea and the water structure. *Journal of Biological Physics*, *27*, 73–79.
de Lima, D. U., & Buckeridge, M. S. (2001). Interaction between cellulose and storage xyloglucans: the influence of the degree of galactosylation. *Carbohydrate Polymers*, *46*, 157–163.
Gidley, M. J., & Bociek, S. M. (1988). Carbon-13CP/MAS NMR studies of amylose inclusion complexes, cyclodextrins, and the amorphous phase of starch granules: relationships between glycosidic linkage conformation and solid-state carbon-13 chemical shifts. *Journal of the American Chemical Society*, *110*, 3820–3829.
Gidley, M., Mcarthur, A., & Underwood, D. (1991). ^{13}C NMR characterization of molecular structures in powders: hydrates and gels of galactomannans and glucomannans. *Food Hydrocolloids*, *5*, 129–140.
Gidley, M. J. (1992). High-resolution solid-state NMR of food materials. *Trends in Food Science & Technology*, *3*, 231–236.
Goycoolea, F. M., Morris, E. R., & Gidley, M. J. (1995). Viscosity of galactomannans at alkaline and neutral pH—evidence of hyperentanglement in solution. *Carbohydrate Polymers*, *27*, 69–71.
Ha, M.-A., Apperley, D. C., & Jarvis, M. C. (1997). Molecular rigidity in dry and hydrated onion cell walls. *Plant Physiology*, *115*, 593–598.
Hayashi, T., Ogawa, K., & Mitsuishi, Y. (1994). Characterisation of the adsorption of xyloglucan to cellulos. *Plant and Cell Physiology*, *35*, 1199–1205.
Heydweiller, A. (1910). Concerning the physical characteristics of solutions in correlation. II. Surface tension and electronic conductivity of watery salt solutions. *Annals of Physics*, *33*, 145–185.
Hofmeister, F. (1888). On the understanding of the effects of salts. *Archiv for Experimentelle Pathologie und Pharmakologie (Leipzig)*, *24*, 247–260.
Kok, M. S., Abdelhameed, A. S., Ang, S., Morris, G. A., & Harding, S. E. (2009). A novel global hydrodynamic analysis of the molecular flexibility of the dietary fibre polysaccharide konjac glucomannan. *Food Hydrocolloids*, *23*, 1910–1917.
Levy, S., York, W. S., Stuikeprill, R., Meyer, B., & Staehelin, L. A. (1991). Simulations of the static and dynamic molecular conformations of xyloglucan—the role of the fucosylated side chain in specific side chain foldin. *Plant Journal*, *1*, 195–215.
Le, B., & Xie, B. (2006). Single molecular chain geometry of konjac glucomannan as a high quality dietary fiber in East Asia. *Food Research International*, *39*, 127–132.
Lima, D. U., Loh, W., & Buckeridge, M. S. (2004). Xyloglucan-cellulose interaction depends on the sidechains and molecular weight of xyloglucan. *Plant Physiology and Biochemistry*, *42*, 389–394.
Ma, X. D., & Pawlik, M. (2007). Intrinsic viscosities and Huggins constants of guar gum in alkali metal chloride solutions. *Carbohydrate Polymers*, *70*, 15–24.
Marchessault, R., Taylor, M., & Winter, W. (1990). ^{13}C CP/MAS NMR spectra of poly-β-D (1 → 4) mannose: mannan. *Canadian Journal of Chemistry*, *68*, 1192–1195.
Mathur, V., & Mathur, N. (2005). Fenugreek and other lesser known legume galactomannan-polysaccharides: scope for developments. *Journal of Scientific and Industrial Research*, *64*, 475.
Mathur, N. (2011). *Industrial galactomannan polysaccharides*. CRC Press.
Mccleary, B. V., Clark, A. H., Dea, I. C. M., & Rees, D. A. (1985). The fine structures of carob and guar galactomannans. *Carbohydrate Research*, *139*, 237–260.
Mcgrane, S. J., Mainwaring, D. E., Cornell, H. J., & Rix, C. J. (2004). The role of hydrogen bonding in amylose gelation. *Starch-Stärke*, *56*, 122–131.
Mezger, T. G. (2006). *The rheology handbook*. Hannover: Vincentz Network.
Mishima, T., Hisamatsu, M., York, W. S., Teranishi, K., & Yamada, T. (1998). Adhesion of beta-D-glucans to cellulose. *Carbohydrate Research*, *308*, 389–395.
Mishra, A., & Malhotra, A. V. (2009). Tamarind xyloglucan: a polysaccharide with versatile application potential. *Journal of Materials Chemistry*, *19*, 8528–8536.
Nagy, N. E., Ballance, S., Kvaalen, H., Fossdal, C. G., Solheim, H., & Hietala, A. M. (2012). Xylem defense wood of Norway spruce compromised by the pathogenic white-rot fungus Heterobasidion parviporum shows a prolonged period of selective decay. *Planta*, *236*, 1125–1133.
Naoi, S., Hatakeyama, T., & Hatakeyama, H. (2002). Phase transition of locust bean gum-: tara gum-and guar gum-water systems. *Journal of Thermal Analysis and Calorimetry*, *70*, 841–852.
Nishinari, K., Takemasa, M., Zhang, H., & Takahashi, R. (2007). Storage plant polysaccharides: xyloglucans, galactomannans, glucomannans. In *Comprehensive glycoscience: from chemistry to systems biology* (1st ed.). Oxford: Elsevier.
Omta, A. W., Kropman, M. F., Woutersen, S., & Bakker, H. J. (2003). Negligible effect of ions on the hydrogen-bond structure in liquid water. *Science*, *301*, 347–349.
Parry, J.-M. (2010). Konjac glucomannan. In A. Imeson (Ed.), *Food stabilisers, thickeners and gelling agents*. Chichester, UK: Wiley-Blackwell.
Penroj, P., Mitchell, J., Hill, S., & Ganjanagunchorn, W. (2005). Effect of konjac glucomannan deacetylation on the properties of gels formed from mixtures of kappa carrageenan and konjac glucomannan. *Carbohydrate Polymers*, *59*, 367–376.
Petkowicz, C., Reicher, F., & Mazeau, K. (1998). Conformational analysis of galactomannans: from oligomeric segments to polymeric chains. *Carbohydrate Polymers*, *37*, 25–39.
Philippova, O. E., Volkov, E. V., Sitnikova, N. L., Khokhlov, A. R., Desbrieres, J., & Rinaudo, M. (2001). Two types of hydrophobic aggregates in aqueous solutions of chitosan and its hydrophobic derivative. *Biomacromolecules*, *2*, 483–490.
Picout, D. R., Ross-Murphy, S. B., Errington, N., & Harding, S. E. (2003). Pressure cell assisted solubilization of xyloglucans: tamarind seed polysaccharide and detarium gum. *Biomacromolecules*, *4*, 799–807.
Putaux, J. (2005). Morphology and structure of crystalline polysaccharides: some recent studies. In *Macromolecular symposia*. pp. 66–71. Wiley Online Library.
Ren, Y., Picout, D. R., Ellis, P. R., & Ross-Murphy, S. B. (2004). Solution properties of the xyloglucan polymer from Afzelia africana. *Biomacromolecules*, *5*, 2384–2391.
Richardson, P. H., Willmer, J., & Foster, T. J. (1998). Dilute solution properties of guar and locust bean gum in sucrose solutions. *Food Hydrocolloids*, *12*, 339–348.
Rieder, A., Knutsen, S. H., Ulset, A.-S. T., Christensen, B. E., Andersson, R., Mikkelson, A., et al. (2015). Inter-laboratory evaluation of SEC-post-column calcofluor for determination of the weight-average molar mass of cereal β-glucan. *Carbohydrate Polymers*, *124*, 254–264.
Russo, D. (2008). The impact of kosmotropes and chaotropes on bulk and hydration shell water dynamics in a model peptide solution. *Chemical Physics*, *345*, 200–211.
Saitô, H., Yokoi, M., & Yamada, J. (1990). Hydration-dehydration-induced conformational changes of agarose: and kappa-and iota-carrageenans as studied by high-resolution solid-state ^{13}C-nuclear magnetic resonance spectroscopy. *Carbohydrate Research*, *199*, 1–10.
Solomon, O., & Ciută, I. (1962). Détermination de la viscosité intrinsèque de solutions de polymères par une simple détermination de la viscosité. *Journal of Applied Polymer Science*, *6*, 683–686.
Song, B. K., Winter, W. T., & Taravel, F. R. (1989). Crystallography of highly substituted galactomannans: fenugreek and lucerne gums. *Macromolecules*, *22*, 2641–2644.
Tatarova, I., Manian, A. P., Siroka, B., & Bechtold, T. (2010). Nonalkali swelling solutions for regenerated cellulose. *Cellulose*, *17*, 913–922.
Tsaih, M. L., & Chen, R. H. (1997). Effect of molecular weight and urea on the conformation of chitosan molecules in dilute solutions. *International Journal of Biological Macromolecules*, *20*, 233–240.
Wang, J., & Somasundaran, P. (2007). Study of galactomannose interaction with solids using AFM: IR and allied techniques. *Journal of Colloid and Interface Science*, *309*, 373–383.
Wang, C., Zhang, Y., Huang, H. X., Chen, M. B., & Li, D. S. (2011). Solution conformation of konjac glucomannan single helix. *Advanced Materials Research*, *197*, 96–104.
Whitney, S. E. C., Brigham, J. E., Darke, A. H., Reid, J. S. G., & Gidley, M. J. (1995). In vitro assembly of cellulose/xyloglucan networks—ultrastructural and molecular aspects. *Plant Journal*, *8*, 491–504.
Whitney, S. E. C., Brigham, J. E., Darke, A. H., Reid, J. S. G., & Gidley, M. J. (1998). Structural aspects of the interaction of mannan-based polysaccharides with bacterial cellulose. *Carbohydrate Research*, *307*, 299–309.
Wiggins, P. (2002). Enzyme reactions and two-state water. *Journal of Biological Physics and Chemistry*, *2*, 25–37.
Williams, M. A. K., Foster, T. J., Martin, D. R., Norton, I. T., Yoshimura, M., & Nishinari, K. (2000). A molecular description of the gelation mechanism of konjac mannan. *Biomacromolecules*, *1*, 440–450.
Wu, Y., Cui, W., Eskin, N., & Goff, H. (2009). An investigation of four commercial galactomannans on their emulsion and rheological properties. *Food Research International*, *42*, 1141–1146.
Yin, W., Zhang, H., Huang, L., & Nishinari, K. (2008). Effects of the lyotropic series salts on the gelation of konjac glucomannan in aqueous solutions. *Carbohydrate Polymers*, *74*, 68–78.
Zhang, Y., & Cremer, P. S. (2006). Interactions between macromolecules and ions: the Hofmeister series. *Current Opinion in Chemical Biology*, *10*, 658–663.